Published in final edited form as:
Cancer Res. 2010 December 1; 70(23): 9703–9710. doi:10.1158/0008-5472.CAN-09-1022.

Genomic instability in mice is greater in Fanconi anemia caused by deficiency of *Fancd2* than *Fancg*

Ramune Reliene[2], **Mitsuko L. Yamamoto**[1], **P. Nagesh Rao**[1], and **Robert H. Schiestl**[1,3,4]

[1] Department of Pathology and Laboratory Medicine, David Geffen School of Medicine, University of California Los Angeles, Los Angeles

[2] Cancer Research Center, Department of Environmental Health Sciences, University at Albany, State University of New York, Albany

[3] Department of Radiation Oncology, David Geffen School of Medicine, University of California Los Angeles, Los Angeles

[4] Department of Environmental Health Sciences, School of Public Health, University of California Los Angeles, Los Angeles

Abstract

Fanconi anemia (FA) results from mutations in the *FANC* genes and is characterized by bone marrow failure, birth defects and a high incidence of cancer. FANCG is a part of the FA core complex that is responsible for monoubiquitination of FANCD2 and FANCI. The precise role of the FA pathway is not well understood, although it may be involved in homologous recombination (HR), non-homologous end joining (NHEJ) and translesion synthesis (TLS). *Fancd2*$^{-/-}$ mice have a more severe phenotype than *Fancg*$^{-/-}$ and other FA core complex deficient mice, although both *Fancg* and *Fancd2* belong to the same FA pathway. We hypothesized that *Fancd2* deficiency results in a more severe phenotype because *Fancd2* also has a FA pathway-independent function in the maintenance of genomic integrity. To test this hypothesis we determined the level of DNA damage and genomic instability in *Fancd2*$^{-/-}$, *Fancg*$^{-/-}$ and wildtype controls. *Fancd2*$^{-/-}$ mice displayed a higher magnitude of chromosomal breakage and micronucleus formation than wildtype or *Fancg*$^{-/-}$ mice. Also, DNA strand breaks were increased in *Fancd2*$^{-/-}$ but not in *Fancg*$^{-/-}$ mice. In addition, *Fancd2*$^{-/-}$ mice displayed an elevated frequency of DNA deletions resulting from HR at the endogenous p^{un} locus. In contrast, in *Fancg*$^{-/-}$ mice, the frequency of DNA deletions was decreased. Thus, *Fancd2* but not *Fancg* deficiency results in elevated chromosomal/DNA breakage and permanent genome rearrangements. This provides evidence that *Fancd2* plays an additional role in the maintenance of genomic stability than *Fancg*, which might explain the higher predisposition to cancer seen in the *Fancd2*$^{-/-}$ mice.

Keywords

Fanconi anemia; mouse; in vivo; homologous recombination; genomic instability

INTRODUCTION

Fanconi anemia (FA) is a rare, recessive (autosomal or X-linked) disorder characterized by progressive bone marrow failure, birth defects, and a markedly increased risk of cancer

Request for reprints: Robert H. Schiestl, Department of Pathology, UCLA School of Medicine, 650 Charles E. Young Drive South, Los Angeles, CA 90024. Phone: 310-267-2087; Fax: 310-267-2578; rschiestl@mednet.ucla.edu.

(1,2). FA patients are particularly susceptible to developing acute myelogenous leukemia, but also develop solid tumors, often squamous cell carcinomas of the head and neck, and gynecological and gastrointestinal systems (3). The most prominent cellular phenotype of FA is hypersensitivity to DNA cross-linking agents, such as cisplatin, mitomycin C and diepoxybutane (4,5). FA cells treated with DNA cross-linking agents display increased chromosomal breakage, radial chromosomes and other cytogenetic abnormalities that are commonly used as diagnostic tests for FA (6). Modestly elevated sensitivity to ionizing radiation (IR) and oxygen has also been observed in cultured FA cells (7,8).

FA is a genetically heterogeneous disease. Currently 13 FA genes (A, B, C, D1, D2, E, F, G, I, J, L, M, and N) have been identified (9–11). Upon DNA damage multiple FANC proteins (FANCA/B/C/E/F/G/L/M and FAAP24/100) form a nuclear core complex that promotes monoubiquitination of the effector protein FANCD2 (12–15). Monoubiquitinated FANCD2 appears during the S-phase of the cell cycle and translocates into the nuclear foci formed at sites of DNA damage (16,17). A recently identified FANCI forms an interdependent complex with FANCD2 and together localize to the nuclear foci following monoubiquitination by the FA core complex (11). The precise functions of FANC proteins are not well understood, although they appear to promote the repair of blocked or broken replication forks by several DNA repair pathways, which include HR, NHEJ and TLS. Co-localization of FANCD2 with HR proteins RAD51, BRCA1 and BRCA2, functional interaction of FANCD2 with BRCA2, and an important finding that the *FANCD1* gene is identical to *BRCA2* suggested the involvement of the FA pathway in HR (16–19). However, because BRCA2-dependent RAD51 nuclear focus formation is not affected in FANCD2 deficient cells and FANCD2 nuclear focus formation is normal in BRCA2 deficient cells, FANCD2 appears to be dispensable for RAD51-dependent HR (20). The role of FANC proteins in HR is difficult to understand, in part due to mixed study results showing that HR in FA cells is decreased (21–24), increased (25,26) or not affected (20). Similarly, the role of the FA pathway in NHEJ is not established given the conflicting results that the FA pathway is either required for the efficient DNA end joining (27,28) or not (21). There is substantial evidence that FANC proteins regulate TLS (23,29). A recent report also suggests that the FA proteins facilitate DNA repair by promoting several pathways, such as HR, NHEJ and TLS (30).

Several mouse models for FA have been generated. These include the FA core complex subunit deficient mice, such as *Fanca*$^{-/-}$, *Fancc*$^{-/-}$ and *Fancg*$^{-/-}$ mice, as well as downstream effector deficient, *Fancd2*$^{-/-}$ mice (31–35). Interestingly, *Fancd2*$^{-/-}$ mice have a more severe phenotype than the FA core complex deficient mice (35). For example, *Fancd2*$^{-/-}$ mice display perinatal lethality, micropthalmia and more severe hypogonadism than FA core complex deficient mice. Most notably, *Fancd2*$^{-/-}$ mice but not *Fanca*$^{-/-}$, *Fancc*$^{-/-}$ or *Fancg*$^{-/-}$ mice are prone to developing epithelial (breast, ovarian and liver) cancers. To understand these differences and further investigate the role of *Fanc* genes in the maintenance of genomic stability we measured and compared DNA damage endpoints in the core complex deficient, *Fancg*$^{-/-}$, mice and the effector subunit deficient, *Fancd2*$^{-/-}$, mice. Namely, we determined the magnitude of chromosomal damage, DNA strand breaks and HR-mediated deletions in the knock-outs and their respective wildtype controls. In most reported studies, HR was measured in the synthetic reporter genes following artificial DNA double strand break (DSB) induction. In contrast to that, we studied spontaneous HR at an endogenous murine locus (36). This assay measures HR between two 70 kb tandem repeats at the p^{un} locus resulting in a deletion of one of the repeats (Fig. 1). Such deletions can occur by several HR subpathways, such as intrachromosomal crossing-over, single-strand annealing, unequal sister chromatid exchange and sister chromatid conversion. The deletion is visualized as a black pigmented cell or a clone thereof on the unpigmented retinal pigment epithelium (RPE) of the eye. We found that the frequency of HR-mediated deletions was

decreased in *Fancg*$^{-/-}$ mice and, in contrast, increased in *Fancd2*$^{-/-}$ mice, as compared to wildtype littermates. In addition, *Fancd2*$^{-/-}$ mice but not *Fancg*$^{-/-}$ mice displayed significantly increased DNA damage and chromosomal instability. This suggests that *Fancd2* has a more important role in the maintenance of genomic stability than *Fancg*.

MATERIALS AND METHODS

Mice

Fancd2 deficient mice were generated in Alan D'Andrea's lab, Dana-Farber Cancer Institute, Harvard Medical School, Boston, USA and were in a mixed genetic background of 129/Sv and C57BL/6J (37)(K. Parmar and A. D'Andrea, unpublished data). *Fancg* deficient mice, were also generated in the same genetic background in Alan D'Andrea's lab (129/Sv and C57BL/6J) (34). C57BL/6Jp^{un}/p^{un} mice were obtained from the Jackson Laboratory (Bar Harbor, ME, USA). The C57BL/6Jp^{un}/p^{un} background is essentially identical to C57BL/6J with an exception of the recessive 70 kb internal duplication in the *pink-eyed dilution* (*p*) gene, termed the *pink-eyed unstable* (p^{un}) allele, resulting in a light gray coat color and pink eyes. The *Fancd2* and *Fancg* mutations were crossed into the C57BL/6Jp^{un}/p^{un} genetic background 3 times. The resulting p^{un}/p^{un} *Fancd2* $^{+/-}$ mice and p^{un}/p^{un} *Fancg*$^{+/-}$ mice had a genetic background containing 93.75% of C57BL/6J and were morphologically similar to the parental C57BL/6Jp^{un}/p^{un} strain. *Fancd2* and *Fancg* deficient mice and wildtype controls were obtained from heterozygous crosses. We also attempted to generate double mutant, *Fancd2*$^{-/-}$*Fancg* $^{-/-}$ mice (by intercrossing double heterozygous *Fancd2* $^{+/-}$ *Fancg*$^{+/-}$mice) but no live double mutant offspring were obtained ($p = 0.01$ as compared with the expected Mendelian segregation, total number of offspring = 99) due to apparent embryonic lethality resulting from combined inactivation of *Fancd2* and *Fancg*.

Mice were bred in an institutional specific pathogen-free (SPF) animal facility under standard conditions with a 12 h light/dark cycle and were given a standard diet (Harlan Teklad No 8656) and water *ad libitum*. Pregnancy was timed by checking for vaginal plugs, with noon of the day of discovery counted as 0.5 days *post coitum* (dpc). Similarly, the time of birth of a litter was timed with the noon of discovery counted as 0.5 days *post partum* (dpp).

Chromosome breakage analysis

Primary fibrobast cultures were established from individual mouse ear clips. The ear clips were rinsed in sterile HBSS supplemented with antibiotics (1% Penn-Strep) media and digested in 2–3 ml of collagenase (500 U/mL) solution at 37°C for up to 120 minutes. The digested cells were washed and plated on in-situ coverslips in RPMI 1640 media containing 10% serum. After 7–10 days of primary growth, standard cytogenetics methods were used to harvest the cells and obtain metaphases. The metaphases cells were analyzed with Giemsa-trypsin (GTG) banding and all available metaphase cells from four dishes were analyzed. The number of these cells varied from each animal but usually ranged from 20–50 in number. Chromosome and chromatid breaks and gaps were scored, recorded and imaged on a Zeiss Axiophot microscope. The total number of cells and breaks/cell analyses were done in a blinded fashion.

In vivo micronucleus assay

The *in vivo* micronucleus assay was performed in normochromatic erythrocytes from peripheral blood (38). Blood was collected from the mouse facial artery and 3 μL was spread onto microscopic slides for staining with Giemsa (Sigma-Aldrich, St. Louis, MO). Two slides per mouse were prepared. In total, 6000 cells per mouse (3000 cells per slide) were analyzed in a blinded fashion.

The comet assay

The comet assay was performed essentially as described elsewhere (39). Blood drawn from the mouse facial artery was diluted 1:50 with phosphate buffered saline (PBS). Sixty μl of blood suspension was mixed with 200 μl of 1% low melting point (LMP) agarose in PBS, ph 7.4, at 37°C and 25 μl aliquots of this mixture were loaded in two replicate molds imprinted on Gelbond film (FMC Bioproducts, Rockport, ME) precoated with 1% normal melting point agarose in PBS. The agarose was allowed to set for 5 min at 4°C and the slides were incubated in lysis solution (2.5 M NaCl, 10 mM Tris, 100 mM Na_2EDTA, pH 10.0, with 1% v/v Triton X-100 and 10% DMSO added fresh) at 4°C for 1 h to remove cellular proteins. The Gelbond film was removed and placed in a horizontal electrophoresis chamber (BioRad, Hercules, CA) filled with fresh, chilled electrophoresis buffer (300 mM NaOH and 1 mM EDTA, ph 13) and left at 4°C for 20 min to allow for DNA unwinding. Electrophoresis then was performed in the same buffer at 20V and 300 mA at 4°C for 40 min. After electrophoresis the Gelbond film was washed three times at 4°C for 5 min each with neutralizing buffer (400 mM Tris-HCl, ph 7.5) before staining with SYBR Gold (1/10,000 dilution of stock solution from Molecular Probes, 495 nm excitation, 537 nm emission). The Gelbond film was rinsed with distilled water and visualized using a fluorescent microscope (Olympus Ax70, Tokyo, Japan; max absorption 495 nm; max emission: 520 nm) through a 10x objective lens. Comet images were captured with a camera (Model 11.2 Color Mosaic, Diagnostic Instruments Inc., USA) and analyzed with the CASP image analysis system (40) (http://casp.sourceforge.net). Several features for each comet were determined including percentage of DNA in the comet tail, tail length, comet length, and tail moment. The tail moment (TM), which is defined as the product of percentage of DNA in the comet tail and tail length, was used to quantify the extent of DNA damage. TM is considered one of the best indices of comet formation by computerized analysis (41). About one hundred randomly captured comets (~ 50 comets on each two replicate molds) per mouse were graded according to degree of damage into 5 classes and given a value 0 – 4 (0, undamaged, 4, maximally damaged). The overall score or damage index for 100 cells can range from 0 (all undamaged) to 400 (all maximally damaged). Because of inter-experimental variability in the background level, the damage index was normalized to a control. The same sex wildtype littermate served as a control for each mutant mouse. Statistical analysis was performed on the actual damage index values prior to data normalization.

HR-mediated deletion assay

We determined the frequency of HR events between two 70 kb DNA repeats in the *pink-eyed unstable* (p^{un}) locus spanning exons 6–18 of the *pink-eyed dilution* (*p*) gene resulting in a deletion of one of the repeats (Fig. 1) (36). The p^{un} allele is reverted to the functional *p* gene by such a deletion event, allowing black pigment accumulation in the cells of the RPE of the eye of developing p^{un}/p^{un} mice. Such HR-mediated deletions or p^{un} reversions can be visualized microscopically after birth, as described in the following section.

Dissection of the retinal pigment epithelium—Offspring were sacrificed at 20 days of age and their eyes were dissected. Whole mount RPE slides were prepared for microscopic analysis of eye-spots. Eyes were processed to expose the RPE layer as previously described (36). The eye was removed from its orbit and immersed in fixative (4 % paraformaldehyde in 0.1 M phosphate buffer, pH 7.4) for one hour and then in PBS until dissection. An incision was made at the upper corneo-scleral border to allow removal of the cornea and lens. To flatten the eye-cup, six to eight incisions were made from the corneo-scleral margin towards the centrally positioned optic nerve, and the dissected eyecup was placed on a glass slide with the retina facing up. The retina was then gently removed and the residual specimen consisting of sclera, choroid and RPE, with the RPE facing up, was mounted in 90% glycerol and visualized under microscope using 10 x objective.

Scoring of HR-mediated deletions visualized as eye-spots—A pigmented cell or a group of adjacent pigmented cells separated from each other by no more than 5 unpigmented cells was considered as one eye-spot that resulted from one HR-mediated deletion (p^{un} reversion) event (42). The number of eye-spots in each RPE was counted. Positions of eye-spots in the RPE were mapped.

The RPE was scanned with a DC120 digital camera (Eastman Kodak Company) mounted on a DMLB microscope (Leica Microsystems, Inc.) using a 2.5 x N-plan objective. The images were assembled and examined in Adobe Photoshop 5.0 on a Macintosh Power Computer. All data were stored and processed with Microsoft Excel.

Distance analysis of eye-spots from the optic nerve—Eye-spots were identified under the microscope and compared with their scanned digital images. Distances were measured with the Adobe Photoshop 5.0 Measurement Tool. Two distances were measured for each eye spot: the *eye-spot distance* is the distance from the center of the optic nerve head to the most proximal edge of the eye-spot, and the *RPE distance* of an eye-spot is the distance from the optic nerve through the eye-spot to the outer edge of the RPE. Dividing the eye-spot distance by the radius gives the proportional distance of each eye spot from the center of the RPE, or its *position*. The position of each eye-spot was determined in this manner to compensate for minor differences in the size of the eyes.

Statistical analysis

Comparison between events in different groups was done by a Student t-test. $P < 0.05$ was considered significant.

RESULTS

Fancd2$^{-/-}$ mice displayed higher frequency of chromosomal breaks than *Fancg*$^{-/-}$ mice

Metaphase spreads of fibroblasts showed that *Fancg*$^{-/-}$ mice had somewhat elevated frequency of chromosomal breaks than wildtype controls but it did not reach statistical significance (Table 1). In contrast, *Fancd2*$^{-/-}$ mice had significantly elevated frequencies of chromosomal breaks as compared to their wildtype controls ($p < 0.0001$). When *Fanc* mutants were compared with one another, *Fancd2*$^{-/-}$ mice had 4.4-fold more chromosomal breaks than *Fancg*$^{-/-}$ mice ($p < 0.001$) (Table 1). Thus, *Fancd2* deficiency resulted in a more pronounced chromosomal instability than *Fancg* deficiency.

Micronucleus formation was increased in *Fancd2*$^{-/-}$mice but not *Fancg*$^{-/-}$ mice

Micronucleus formation was determined in normochromatic peripheral blood erythrocytes, as a measure of chromosomal damage. *Fancg*$^{-/-}$ mice had 23% more micronuclei than *Fancg*$^{+/+}$ mice, but was not significantly increased ($p > 0.05$) (Fig. 2). The difference was also not statistically significant when both wildtype controls (*Fancg*$^{+/+}$ and *Fancd2*$^{+/+}$)were combined into one control group. In contrast, the micronucleus frequency was significantly increased (by 40%) in *Fancd2*$^{-/-}$ mice compared with *Fancd2*$^{+/+}$ mice ($p < 0.05$) and combined controls ($p < 0.01$) (Fig. 2). Although, *Fancg* deficient mice displayed a somewhat increased frequency of micronuclei, *Fancd2* deficiency led to a more severe chromosomal damage than *Fancg* deficiency, similar to chromosomal breakage data reported here.

DNA strand breaks were increased in *Fancd2*$^{-/-}$ but not in *Fancg*$^{-/-}$mice

DNA strand breaks were determined by the alkaline comet assay in whole blood collected from *Fancg*$^{-/-}$ and *Fancd2*$^{-/-}$ mice and respective wildtype littermate controls. *Fancg*$^{-/-}$

micehad a similar frequency of DNA strand breaks as *Fancg*$^{+/+}$ mice(Fig. 3). *Fancd2*$^{-/-}$ micehad 1.8-fold more breaks than their respective wildtype controls and *Fancg*$^{-/-}$ mice (Fig. 3). This observation is consistent with the data from Table 1 and Fig. 2 showing that *Fancd2* deficiency has a more severe phenotype in terms of DNA damage than *Fancg* deficiency.

HR-mediated deletions were increased in *Fancd2*$^{-/-}$ mice and decreased in *Fancg*$^{-/-}$ mice

The frequency of HR events resulting in 70 kb DNA deletions was determined in *Fancg*$^{-/-}$ mice, *Fancd2*$^{-/-}$ mice and wildtype littermate controls as the number of eye-spots per RPE (Fig. 4). The frequency of eye-spots was reduced by 36% in *Fancg*$^{-/-}$ mice ($p < 0.001$) and, in contrast, increased by 30% in *Fancd2*$^{-/-}$ mice ($p < 0.01$) compared to respective wildtype littermates. When *Fanc* mutants were compared with each other, *Fancd2*$^{-/-}$ mice had 48% more eye-spots than *Fancg*$^{-/-}$ mice ($p < 0.001$).

Because the number of eye-spots did not differ significantly between *Fancg*$^{+/+}$ and *Fancd2*$^{+/+}$ mice, they were combined into one control group. When compared to combined wildtype controls, *Fancg*$^{-/-}$ mice still had significantly fewer eye-spots ($p < 0.001$) and *Fancd2*$^{-/-}$ significantly more ($p < 0.01$). The average number of eye-spots/RPE was 6.35 ± 0.34 (n = 57), 4.27 ± 0.28 (n = 30) and 8.25 ± 0.6 (n = 20) in combined wildtype controls, *Fancg*$^{-/-}$ mice and *Fancd2*$^{-/-}$ mice, respectively.

These findings demonstrated that a deficiency in *Fancg* versus *Fancd2* has different consequences in spontaneous HR involving direct repeats: *Fancg* deficiency reduces HR resulting in the frequency of deletions below the normal range, while *Fancd2* deficiency increases HR resulting in elevated frequency of permanent genome rearrangements (i.e. DNA deletions).

Positional distribution of HR-mediated deletions in *Fancg*$^{-/-}$ and *Fancd2*$^{-/-}$ deficient mice

The mouse RPE develops during a second half of gestation in a radial pattern, away from the optic nerve head to the edge of the RPE (Fig. 1) (36). We mapped relative positions of eye-spots within the RPE to determine the approximate time during embryo development at which an HR event occurred (36). For that we divided the RPE into 10 concentric regions. The concentric region closest to the optic nerve head, '0.0–0.1', corresponds to the beginning of the RPE development, while the most remote region, '0.9–1.0', indicates the end of RPE development (Fig. 1). We determined the position of eye-spots in the RPE of *Fancg*$^{-/-}$ mice, *Fancd2*$^{-/-}$ mice and wildtype littermate controls. *Fancg*$^{-/-}$ mice had fewer eye-spots than *Fancg*$^{+/+}$ mice in most (9 of 10) regions of the RPE (Fig. 5*A*). In contrast, *Fancd2*$^{-/-}$ mice had more eye-spots than *Fancd2*$^{+/+}$ mice in most regions of the RPE (Fig. 5*B*). The same pattern was observed when mutant mice were compared with a combined wildtype control. When mutants were compared with each other, *Fancd2*$^{-/-}$ mice had ~2-fold (2.3 ± 0.4) more eye-spots in a given RPE region than *Fancg*$^{-/-}$ mice in most (8 of 10) regions. Thus, in *Fancg*$^{-/-}$ mice, HR was reduced and, in *Fancd2*$^{-/-}$ mice, HR was increased continuously during RPE development.

DISCUSSION

Non-epistatic interaction of *Fancg* and *Fancd2*

We found that mice deficient in the FA core complex subunit, *Fancg*, and the downstream effector, *Fancd2*$^{-/-}$, have distinct phenotypes in terms of spontaneous chromosomal instability and HR. Chromosomal and DNA damage was significantly elevated in *Fancd2*$^{-/-}$ but not *Fancg*$^{-/-}$mice. Also, the outcome of HR at the endogenous p^{un} locus was different: HR-mediated deletions were increased in *Fancd2*$^{-/-}$ mice and reduced in *Fancg*$^{-/-}$ mice. In

this study, we also attempted to produce double mutant mice but encountered embryonic lethality (data not shown). These findings were unexpected given that both *Fancg* and *Fancd2* are the members of the FA pathway and a deficiency in one or another gene or both genes of the same pathway presumably leads to similar outcomes. The observed differences reported here suggest that *Fancg* and *Fancd2* are non-epistatic genes. That is the Fancd2 protein plays another role in the maintenance of genomic stability than just being a downstream effector of the FA pathway. In support of this notion, it has been demonstrated in tissue culture experiments that FANCD2 participates in the intra S-phase checkpoint in an FA core complex-independent manner in response to IR (43). FANCD2 is phosphorylated by ATM to halt DNA replication. *FANCD2* deficient cells display radioresistant DNA synthesis, a phenotype of *ATM* deficient cells, while other FA complementation groups do not (43). Thus, pronounced chromosomal damage and hyperrecombination in *Fancd2*$^{-/-}$ mice observed in this study may result from an intra S-phase checkpoint defect. In support of this, elevated HR at the p^{un} locus has also been observed in mice characterized by impaired cell cycle checkpoint control, such as *Atm* and *p53* deficient mice (44).

Fancd2 may also have other functions that are independent of the FA core complex. It has been demonstrated that unmodified Fancd2 binds directly and specifically to DNA double strand ends and Holliday junctions *in vitro* (45). *Fancg*$^{-/-}$ mice contain non-ubiquitinated Fancd2 protein (34), which would allow for the latter Fancd2-DNA interaction. However it's not clear if unmodified Fancd2 binds directly to DNA double strand breaks and/or enhances its repair *in vivo*. On the other hand, Fancd2 can be modified by other cellular proteins. In particular, Fancd2 is subject to phosphorylation by CHK1 kinase (46). This phosphorylation occurs independently of the FA core complex and is important for interaction with BRCA2 (46). It's tempting to speculate that Fancd2 plays a role in the maintenance of genomic stability through interactions with DNA or other DNA repair proteins, however, further studies are needed to characterize the FA-pathway independent *Fancd2* functions.

Taken together, the observed phenotypic differences in *Fancd2*$^{-/-}$ and *Fancg*$^{-/-}$ mice and embryonic lethality of double mutant mice suggest a non-epistatic interaction between *Fancg* and *Fancd2*.

Comparison of HR assays in our and other studies

The mild defect in HR in *Fancg*$^{-/-}$ mice in our study is in agreement with studies that showed reduced HR repair of I-SceI generated DNA DSBs in chromosomally integrated substrates in FA patient-derived *FANCG* cell lines (21) and *Fancg* deficient chicken DT40 cells (22). In contrast, increased HR in *Fancd2*$^{-/-}$ mice observed in this study conflicts with the studies reporting that HR repair in *FANCD2* deficient cells is either decreased (21,24) or unaffected (20). However, these findings are difficult to compare given that not only different experimental systems but also different HR assays were used. The published studies were carried out in experimental systems ranging from chicken DT40 cells (24) to FA patient derived cells (20,21), while our study was done in knock-out mice. Also, previous studies measured the repair of DSBs generated by I-SceI enzyme in the synthetic reporter genes, while, in the current study we determined frequencies of spontaneous HR events at the endogenous murine p^{un} locus. The previously reported HR assays measure repair of a very specific subset of DNA damage, namely repair of a DSB following enzymatic digestion, while the HR assay used in this study can detect a wider variety of DNA strand breaks including those caused by oxidative stress and replication fork arrest.

The high frequency of DNA breaks found in *Fancd2*$^{-/-}$ mice can promote recombination resulting in deletions. This is a likely scenario in *Fancd2*$^{-/-}$ mice. The Fancd2 protein seems to be dispensable to complete HR processes under these circumstances (high chromosomal/

DNA instability). In *Fancg*$^{-/-}$ mice, the lower frequency of DNA strand breaks was associated with lower frequency of deletions. In fact, the deletion frequency fell below the normal range possibly because of a mild defect in the HR machinery. Thus, the role of Fanconi genes, *Fancd2* and *Fancg*, in the HR outcome may depend on the frequency of DNA strand breaks.

Hyperrecombination in *Fancd2* deficient mice may play a role in carcinogenesis

Mouse models for FA revealed that *Fancd2*$^{-/-}$ mice have a more severe phenotype than the FA core complex deficient mice, such as *Fanca*$^{-/-}$, *Fancc*$^{-/-}$ and *Fancg*$^{-/-}$ mice (35). Most notably, *Fancd2* deficient mice but not *Fancg* deficient have an increased incidence of epithelial cancers, such as breast, ovarian and liver cancers. In this study, *Fancd2*$^{-/-}$ mice displayed elevated chromosomal instability and an increased frequency of HR-mediated DNA deletions. In contrast, *Fancg*$^{-/-}$ mice did not show significantly increased genomic instability. Therefore the elevated frequency of chromosomal damage and aberrant HR resulting in DNA deletions may play a role in carcinogenesis in *Fancd2* deficient mice. Chromosomal instability and abnormally increased HR has been associated with carcinogenesis in experimental systems and human cancer-prone syndromes (47,48). For example, cancer-prone *Atm* deficient mice and p53 deficient mice display a hyperrecombination phenotype at the same genomic locus and to similar extent as *Fancd2* deficient mice in this study (44). Thus, the observed aberrant HR may account for cancer development in *Fancd2*$^{-/-}$ mice.

Acknowledgments

Fancg and *Fancd2* deficient mice were a gift from Alan D'Andrea. This research was supported by NIH, RO1 grant No. ES09519 to RHS and NIH 1RO3 CA133928-01 to RR.

References

1. Joenje H, Patel KJ. The emerging genetic and molecular basis of Fanconi anaemia. Nat Rev Genet. 2001; 2:446–57. [PubMed: 11389461]
2. Bogliolo M, Cabre O, Callen E, et al. The Fanconi anaemia genome stability and tumour suppressor network. Mutagenesis. 2002; 17:529–38. [PubMed: 12435850]
3. Rosenberg PS, Greene MH, Alter BP. Cancer incidence in persons with Fanconi anemia. Blood. 2003; 101:822–6. [PubMed: 12393424]
4. Sasaki MS, Tonomura A. A high susceptibility of Fanconi's anemia to chromosome breakage by DNA cross-linking agents. Cancer Res. 1973; 33:1829–36. [PubMed: 4352739]
5. German J, Schonberg S, Caskie S, Warburton D, Falk C, Ray JH. A test for Fanconi's anemia. Blood. 1987; 69:1637–41. [PubMed: 3107630]
6. Auerbach AD. Fanconi anemia diagnosis and the diepoxybutane (DEB) test. Exp Hematol. 1993; 21:731–3. [PubMed: 8500573]
7. Gluckman E. Radiosensitivity in Fanconi anemia: application to the conditioning for bone marrow transplantation. Radiother Oncol. 1990; 18 (Suppl 1):88–93. [PubMed: 2247653]
8. Saito H, Hammond AT, Moses RE. Hypersensitivity to oxygen is a uniform and secondary defect in Fanconi anemia cells. Mutat Res. 1993; 294:255–62. [PubMed: 7692265]
9. Taniguchi T, D'Andrea AD. Molecular pathogenesis of Fanconi anemia: recent progress. Blood. 2006; 107:4223–33. [PubMed: 16493006]
10. Reid S, Schindler D, Hanenberg H, et al. Biallelic mutations in PALB2 cause Fanconi anemia subtype FA-N and predispose to childhood cancer. Nat Genet. 2007; 39:162–4. [PubMed: 17200671]
11. Smogorzewska A, Matsuoka S, Vinciguerra P, et al. Identification of the FANCI Protein, a Monoubiquitinated FANCD2 Paralog Required for DNA Repair. Cell. 2007; 129:289–301. [PubMed: 17412408]

12. Thompson LH. Unraveling the Fanconi anemia-DNA repair connection. Nat Genet. 2005; 37:921–2. [PubMed: 16132046]
13. Niedernhofer LJ, Lalai AS, Hoeijmakers JH. Fanconi anemia (cross)linked to DNA repair. Cell. 2005; 123:1191–8. [PubMed: 16377561]
14. Ciccia A, Ling C, Coulthard R, et al. Identification of FAAP24, a Fanconi anemia core complex protein that interacts with FANCM. Mol Cell. 2007; 25:331–43. [PubMed: 17289582]
15. Ling C, Ishiai M, Ali AM, et al. FAAP100 is essential for activation of the Fanconi anemia-associated DNA damage response pathway. Embo J. 2007; 26:2104–14. [PubMed: 17396147]
16. Taniguchi T, Garcia-Higuera I, Andreassen PR, Gregory RC, Grompe M, D'Andrea AD. S-phase-specific interaction of the Fanconi anemia protein, FANCD2, with BRCA1 and RAD51. Blood. 2002; 100:2414–20. [PubMed: 12239151]
17. Wang X, Andreassen PR, D'Andrea AD. Functional interaction of monoubiquitinated FANCD2 and BRCA2/FANCD1 in chromatin. Mol Cell Biol. 2004; 24:5850–62. [PubMed: 15199141]
18. Wang X, D'Andrea AD. The interplay of Fanconi anemia proteins in the DNA damage response. DNA Repair (Amst). 2004; 3:1063–9. [PubMed: 15279794]
19. Howlett NG, Taniguchi T, Olson S, et al. Biallelic inactivation of BRCA2 in Fanconi anemia. Science. 2002; 297:606–9. [PubMed: 12065746]
20. Ohashi A, Zdzienicka MZ, Chen J, Couch FJ. Fanconi anemia complementation group D2 (FANCD2) functions independently of BRCA2- and RAD51-associated homologous recombination in response to DNA damage. J Biol Chem. 2005; 280:14877–83. [PubMed: 15671039]
21. Nakanishi K, Yang YG, Pierce AJ, et al. Human Fanconi anemia monoubiquitination pathway promotes homologous DNA repair. Proc Natl Acad Sci U S A. 2005; 102:1110–5. [PubMed: 15650050]
22. Yamamoto K, Ishiai M, Matsushita N, et al. Fanconi anemia FANCG protein in mitigating radiation- and enzyme-induced DNA double-strand breaks by homologous recombination in vertebrate cells. Mol Cell Biol. 2003; 23:5421–30. [PubMed: 12861027]
23. Niedzwiedz W, Mosedale G, Johnson M, Ong CY, Pace P, Patel KJ. The Fanconi anaemia gene FANCC promotes homologous recombination and error-prone DNA repair. Mol Cell. 2004; 15:607–20. [PubMed: 15327776]
24. Seki S, Ohzeki M, Uchida A, et al. A requirement of FancL and FancD2 monoubiquitination in DNA repair. Genes Cells. 2007; 12:299–310. [PubMed: 17352736]
25. Thyagarajan B, Campbell C. Elevated homologous recombination activity in fanconi anemia fibroblasts. J Biol Chem. 1997; 272:23328–33. [PubMed: 9287344]
26. Donahue SL, Lundberg R, Saplis R, Campbell C. Deficient regulation of DNA double-strand break repair in Fanconi anemia fibroblasts. J Biol Chem. 2003; 278:29487–95. [PubMed: 12748186]
27. Lundberg R, Mavinakere M, Campbell C. Deficient DNA end joining activity in extracts from fanconi anemia fibroblasts. J Biol Chem. 2001; 276:9543–9. [PubMed: 11124945]
28. Donahue SL, Campbell C. A DNA double strand break repair defect in Fanconi anemia fibroblasts. J Biol Chem. 2002; 277:46243–7. [PubMed: 12361951]
29. Mirchandani KD, McCaffrey RM, D'Andrea AD. The Fanconi anemia core complex is required for efficient point mutagenesis and Rev1 foci assembly. DNA Repair (Amst). 2008; 7:902–11. [PubMed: 18448394]
30. Hinz JM, Nham PB, Urbin SS, Jones IM, Thompson LH. Disparate contributions of the Fanconi anemia pathway and homologous recombination in preventing spontaneous mutagenesis. Nucleic Acids Res. 2007; 35:3733–40. [PubMed: 17517774]
31. Cheng NC, van de Vrugt HJ, van der Valk MA, et al. Mice with a targeted disruption of the Fanconi anemia homolog Fanca. Hum Mol Genet. 2000; 9:1805–11. [PubMed: 10915769]
32. Wong JC, Alon N, McKerlie C, Huang JR, Meyn MS, Buchwald M. Targeted disruption of exons 1 to 6 of the Fanconi Anemia group A gene leads to growth retardation, strain-specific microphthalmia, meiotic defects and primordial germ cell hypoplasia. Hum Mol Genet. 2003; 12:2063–76. [PubMed: 12913077]
33. Koomen M, Cheng NC, van de Vrugt HJ, et al. Reduced fertility and hypersensitivity to mitomycin C characterize Fancg/Xrcc9 null mice. Hum Mol Genet. 2002; 11:273–81. [PubMed: 11823446]

34. Yang Y, Kuang Y, Montes De Oca R, et al. Targeted disruption of the murine Fanconi anemia gene, Fancg/Xrcc9. Blood. 2001; 98:3435–40. [PubMed: 11719385]
35. Houghtaling S, Timmers C, Noll M, et al. Epithelial cancer in Fanconi anemia complementation group D2 (Fancd2) knockout mice. Genes Dev. 2003; 17:2021–35. [PubMed: 12893777]
36. Reliene R, Bishop AJ, Aubrecht J, Schiestl RH. In vivo DNA deletion assay to detect environmental and genetic predisposition to cancer. Methods Mol Biol. 2004; 262:125–39. [PubMed: 14769959]
37. Kim JM, Parmar K, Huang M, et al. Inactivation of murine Usp1 results in genomic instability and a fanconi anemia phenotype. Dev Cell. 2009; 16:314–20. [PubMed: 19217432]
38. Hayashi M, Tice RR, MacGregor JT, et al. In vivo rodent erythrocyte micronucleus assay. Mutat Res. 1994; 312:293–304. [PubMed: 7514741]
39. McNamee JP, McLean JR, Ferrarotto CL, Bellier PV. Comet assay: rapid processing of multiple samples. Mutat Res. 2000; 466:63–9. [PubMed: 10751727]
40. Konca K, Lankoff A, Banasik A, et al. A cross-platform public domain PC image-analysis program for the comet assay. Mutat Res. 2003; 534:15–20. [PubMed: 12504751]
41. McKelvey-Martin VJ, Green MH, Schmezer P, Pool-Zobel BL, De Meo MP, Collins A. The single cell gel electrophoresis assay (comet assay): a European review. Mutat Res. 1993; 288:47–63. [PubMed: 7686265]
42. Reliene R, Bishop AJ, Li G, Schiestl RH. Ku86 deficiency leads to reduced intrachromosomal homologous recombination in vivo in mice. DNA Repair (Amst). 2004; 3:103–11. [PubMed: 14706343]
43. Taniguchi T, Garcia-Higuera I, Xu B, et al. Convergence of the fanconi anemia and ataxia telangiectasia signaling pathways. Cell. 2002; 109:459–72. [PubMed: 12086603]
44. Bishop AJ, Hollander MC, Kosaras B, Sidman RL, Fornace AJ Jr, Schiestl RH. Atm-, p53-, and Gadd45a-deficient mice show an increased frequency of homologous recombination at different stages during development. Cancer Res. 2003; 63:5335–43. [PubMed: 14500365]
45. Park WH, Margossian S, Horwitz AA, Simons AM, D'Andrea AD, Parvin JD. Direct DNA binding activity of the Fanconi anemia D2 protein. J Biol Chem. 2005; 280:23593–8. [PubMed: 15849361]
46. Zhi G, Wilson JB, Chen X, et al. Fanconi anemia complementation group FANCD2 protein serine 331 phosphorylation is important for fanconi anemia pathway function and BRCA2 interaction. Cancer Res. 2009; 69:8775–83. [PubMed: 19861535]
47. Bishop AJ, Schiestl RH. Homologous recombination as a mechanism for genome rearrangements: environmental and genetic effects. Hum Mol Genet. 2000; 9:2427–334. [PubMed: 11005798]
48. Reliene R, Bishop AJ, Schiestl RH. Involvement of homologous recombination in carcinogenesis. Adv Genet. 2007; 58:67–87. [PubMed: 17452246]

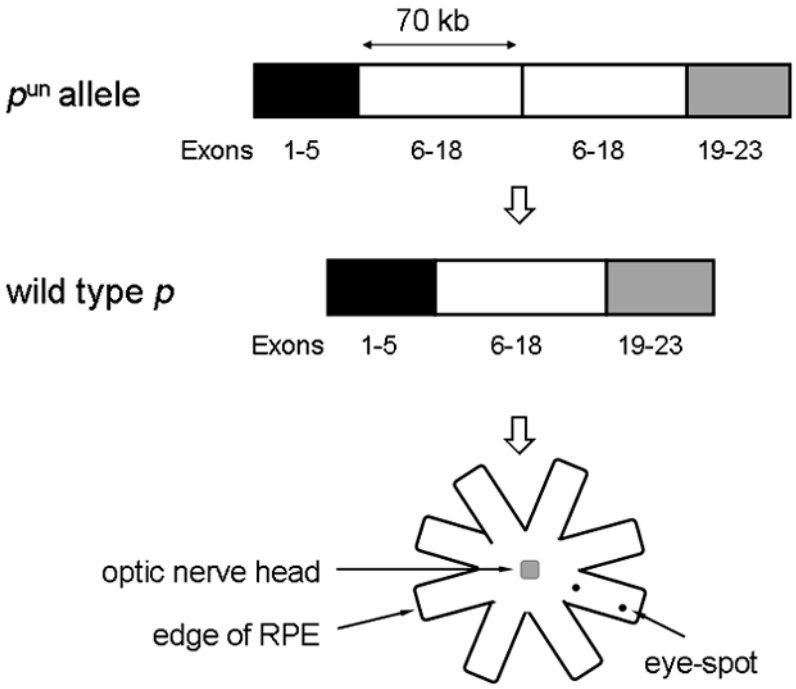

Figure 1.
Homologous recombination leading to a DNA deletion in the murine p^{un} locus. A 70 kb deletion spanning exons 6–18 reconstitutes the wildtype *p* gene, which results in black pigment accumulation in the affected cells of RPE of the developing mouse. Schematic representation of the p^{un} locus and dissected RPE is shown.

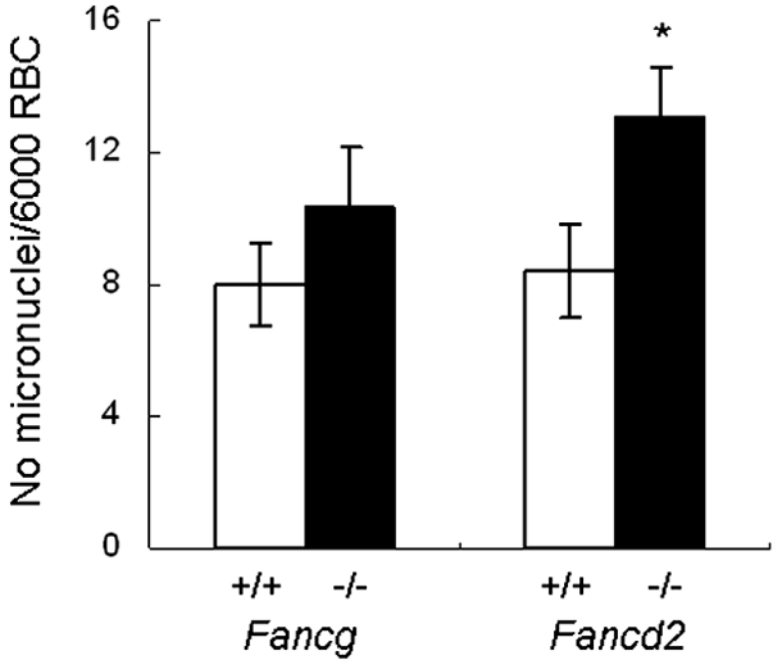

Figure 2.

The frequency of micronucleus formation in *Fancg* deficient mice, *Fancd2* deficient mice and respective wildtype controls. Mean ± SEM (error bars) is shown, n = 7, $Fancg^{+/+}$, n = 8, $Fancg^{-/-}$, n = 7, $Fancd2^{+/+}$, n = 8, $Fancd2^{-/-}$ mice, *, $p < 0.05$, compared to respective wildtype controls. In total 6000 RBC/mouse were analyzed.

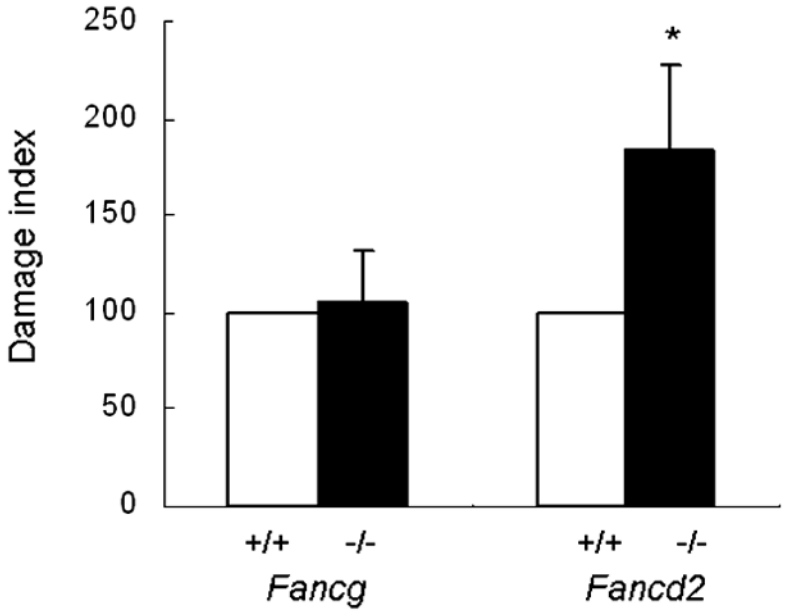

Figure 3.

The frequency of DNA strand breaks in *Fancg* deficient mice, *Fancd2* deficient mice and respective wildtype controls. Mean ± SEM (error bars) is shown, n = 5 mice per genotype, *, $p < 0.05$, compared to the respective wildtype control. Damage index was calculated using TM and was normalized to controls.

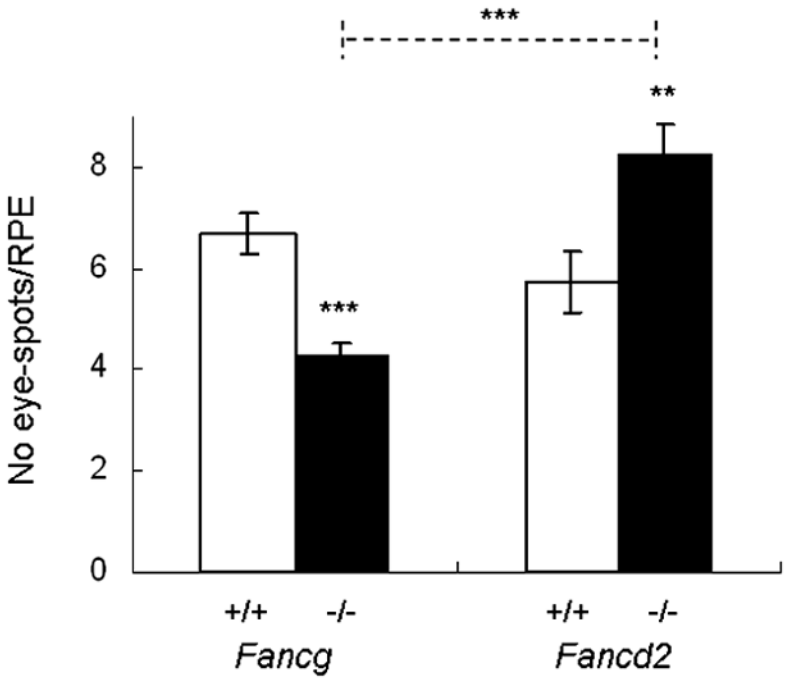

Figure 4.

The frequency of eye-spots in the RPE of *Fancg* deficient mice, *Fancd2* deficient mice and respective wildtype controls. Mean ± SEM (error bars) is shown: n= 37, $Fancg^{+/+}$, n = 30, $Fancg^{-/-}$, n = 20, $Fancd2^{+/+}$, n = 20, $Fancd2^{-/-}$ RPEs. ***, p< 0.001, **, < 0.01 compared to respective control. A dashed line indicates a significant difference (***, p< 0.001) between $Fancg^{-/-}$ and $Fancd2^{-/-}$ mice.

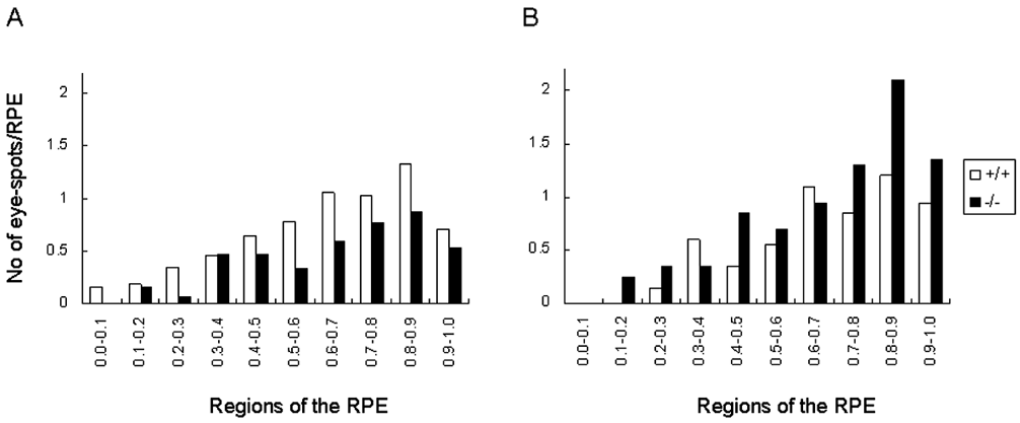

Figure 5.

Positional distribution of eye-spots in the RPE of *Fancg* deficient mice (A) and *Fancd2* deficient mice (B) and their respective controls. Mutant mice are indicated in black bars, wildtype controls are shown in open bars.

Table 1

Chromosomal breakage analysis in *Fancg*$^{-/-}$ and *Fancd2*$^{-/-}$ mice.

Genotype	Chromosomal breaks per cell	number of mice	P, mutant vs. wildtype
Fancg$^{-/-}$	0.26 ± 0.25	4	NS
Fancg$^{+/+}$	0	3	
Fancd2$^{-/-}$	1.15 ± 0.12	4	< 0.0001
Fancd2$^{+/+}$	0	3	

Mean ± SD is shown; $p < 0.001$, *Fancg*$^{-/-}$ versus *Fancd2*$^{-/-}$ mice; NS, not significant